

1

2

*Paleoceanography*

3

Supporting Information for

4

**Calibration of the B/Ca proxy in the planktic foraminifer *Orbulina universa* to  
Paleocene seawater conditions**

5

6

7

Laura L. Haynes<sup>1,2</sup>, Bärbel Hönisch<sup>1,2</sup>, Kelsey Dyez<sup>1</sup>, Kate Holland<sup>3</sup>, Yair Rosenthal<sup>4,5</sup>,  
Carina R. Fish<sup>6</sup>, Adam V. Subhas<sup>7</sup>, James W. B. Rae<sup>8,9</sup>

8

9

10

<sup>1</sup>Lamont-Doherty Earth Observatory of Columbia University, Palisades, NY <sup>2</sup>Department of  
Earth and Environmental Sciences, Columbia University, NY, NY <sup>3</sup>Research School of Earth  
Sciences, The Australian National University, Canberra, ACT <sup>4</sup>Institute for Marine Sciences,  
Rutgers University, New Brunswick, NJ <sup>5</sup>Department of Earth and Planetary Sciences, Rutgers  
University, New Brunswick, NJ <sup>6</sup>Department of Earth and Planetary Sciences, University of  
California, Davis, CA <sup>7</sup>Division of Geological and Planetary Sciences, California Institute of  
Technology, Pasadena, CA <sup>8</sup>Bristol Isotope Group, University of Bristol, UK <sup>9</sup>Department of  
Earth and Environmental Sciences, University of St. Andrews, UK

11

12

13

14

15

16

17

18

**Contents of this file**

19

20

21

22

Text S1 to S6

Figures S1 to S7

Tables S1, S4, S5

23

**Introduction**

24

This supplementary material includes details on calculations performed in this study, auxiliary  
culture data, and the methodology for the measurement of foraminiferal shell surface area.  
Growth rate estimates, individual and average shell weights, and all culture experiment  
parameters are reported. The sequence of steps for calculating carbonate system variables at the  
PETM is detailed. We also provide the output for our calibration scenario in which we use  
measured B/Ca and our new “Paleocene” calibrations to calculate total dissolved inorganic  
carbon (DIC) across the PETM excursion. Trace element data for a comparison between  
foraminifers that were terminated prior to gametogenesis versus foraminifers that completed the  
life cycle are also reported. Finally, we detail the results of an alternate calibration scenario  
explored in the main text.

25

26

27

28

29

30

31

32

33

34

35

36

37

38

## 39 S1. Methodology for B/Ca Measurements at the Bristol Isotope Group

40 In addition to the culture data from 2013 (Santa Catalina Island) and 2015 (Puerto  
41 Rico), we also report here a previously unpublished pH calibration for B/Ca in *O.*  
42 *universa* from the Puerto Rico field site for accurate comparison to our data collected  
43 there (Table S2, Figure S1). These pH experiments, cultured at Puerto Rico in 2010, were  
44 analyzed at the Bristol Isotope Laboratory. Foraminiferal cleaning procedures follow  
45 Rae et al. (2011) and Henehan et al. (2015), and are identical to those described in the  
46 main text, but with an oxidative cleaning solution of 1% H<sub>2</sub>O<sub>2</sub> buffered with 0.1 M  
47 NH<sub>4</sub>OH, and dissolution in 0.075 M HNO<sub>3</sub>. These samples were analyzed on an Element  
48 2 SF-ICP-MS by sample-standard bracketing following Foster (2008), with samples  
49 diluted in 0.5 M HNO<sub>3</sub> and matrix-matched to the same Ca concentration as the standards  
50 (3 mM Ca). Long term 2 RSD reproducibility of secondary standards, consisting of  
51 solutions with similar elemental compositions to dissolved carbonates, is <5 % for B/Ca  
52 and <3 % for Mg/Ca. Bracketing standards were calibrated to standards used at Rutgers  
53 University, minimizing inter-laboratory bias between these labs.

54

55

56

57

58

59

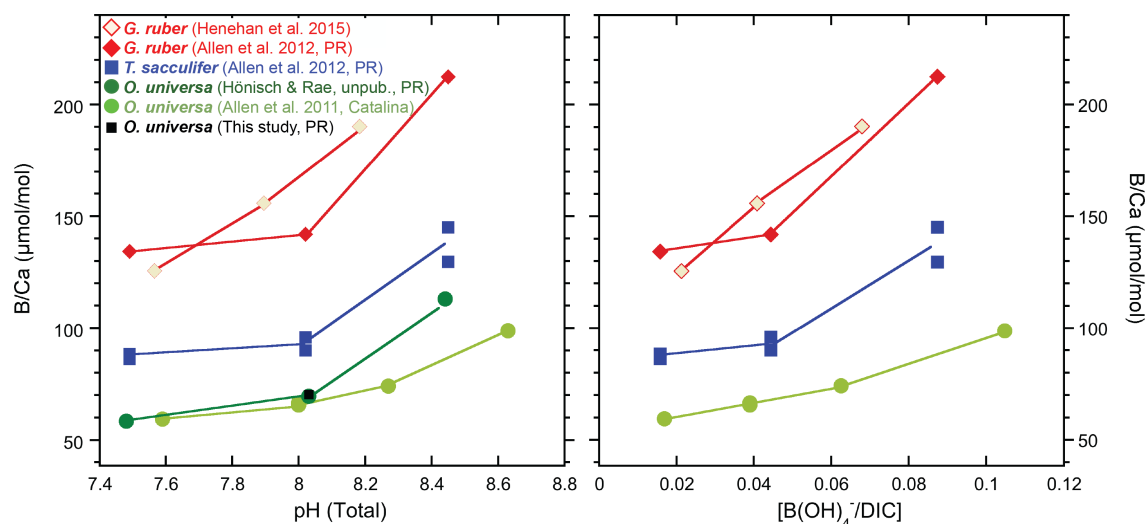
60

61

62

63

64



65 Figure S1. The sensitivity of B/Ca to pH and [B(OH)<sub>4</sub><sup>-</sup>]/DIC in pH culture experiments  
66 from Allen et al. (2011, 2012) and Henehan et al. (2015) and this study. *Globigerinoides*  
67 *ruber* (red) records the highest overall B/Ca values, and shows the highest sensitivity to  
68 pH. The ambient data from the Puerto Rico 2015 season (BH6, this study) are shown as  
69 black squares and agree well with data of the Puerto Rico 2010 pH calibration, measured  
70 at Bristol. The pH calibration for *O. universa* from Puerto Rico is shown in dark green,  
71 and appears to have a higher sensitivity than *O. universa* from Catalina, though this is  
72 mostly driven by by the high pH experiment.

73

## 74 S2. Estimation of Growth Rate from Brunauer-Emmett-Teller Measurements

75 We estimated average foraminifer shell growth rates for each of our foraminifers in  
76 culture from weight and duration of sphere thickening data. To find area-normalized

77 growth rates for comparison to inorganic calcites, however, we need to estimate the  
78 surface area of each spherical shell in addition to growth rates in  $\mu\text{g}/\text{day}$ . To estimate  
79 shell surface area, we use Brunauer-Emmett-Teller (BET) measurements of pooled fossil  
80 *O. universa* shell samples in the 425-515, 515-600, and 600-865  $\mu\text{m}$  size fractions of Fish  
81 et al. (in prep.) to estimate the approximate corresponding surface area of cultured  
82 foraminifer shells in these given size fractions. Samples were collected from a sub-core  
83 of R/V SONNE SO164-17-1 box core within the Florida Straits (Lat: 24°04,93N Long:  
84 80°52,89W, water depth 952 m). Core-top samples were washed, sieved, and picked for  
85 *O. universa* in the above size fractions. BET measurements were made at USC on  
86 samples of pooled foraminifer shells using a Micromeritics ASAP 2010 instrument and  
87 Kr as the analysis gas (de Kanel and Morse, 1979; Subhas et al., 2015). The number of  
88 individuals included in each sample ranged from 110-380, depending on the size fraction  
89 and the associated surface area based on the required amount of  $\geq 0.05 \text{ m}^2$  surface area  
90 per sample. Surface area measurements for each pooled sample yield results in  $\text{m}^2/\text{g}$ . To  
91 find the surface area of an average individual shell in each BET sample, we first divided  
92 the weight of the BET sample by the number of individuals included to find the average  
93 shell weight (Table S1). Then, the average shell weight was multiplied by the average  
94 BET-derived surface area in  $\text{m}^2/\text{g}$  to find the average individual shell surface area in this  
95 size fraction. We then applied these averages to our cultured foraminifer shells based on  
96 their final measured size. For example, a cultured foraminifer with a diameter of 500  $\mu\text{m}$   
97 was assumed to have the average surface area of a foraminifer from the 425-515  $\mu\text{m}$  size  
98 fraction BET sample.

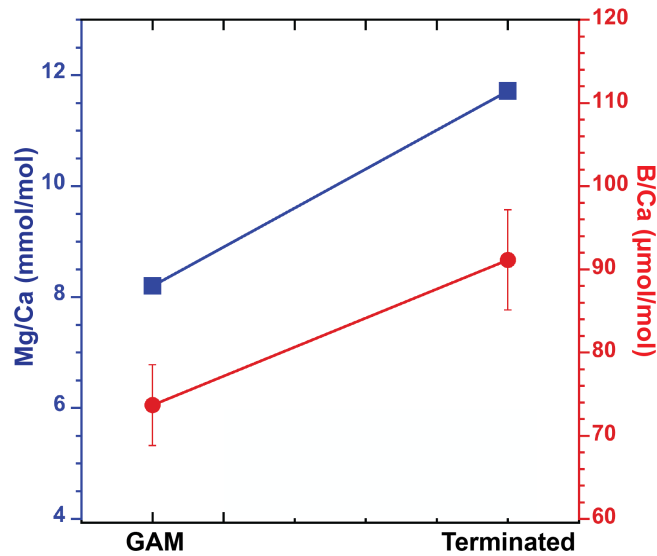
99

### 100 **S3. Effects of Using Pre-Gametogenic (Terminated) Foraminifers and Implications** 101 **for Catalina Low Light Experiments**

102 Out of 19 total foraminifers in our low light experimental sample from Catalina Island we  
103 included one foraminifer that was terminated prior to gametogenesis. To assess the trace  
104 element signature of pre-gametogenic foraminifers, we conducted a paired trace element  
105 analysis of gametogenic and pre-gametogenic foraminifera from the same experiment in  
106 Puerto Rico (BH7, Table S4). We found that both B/Ca and Mg/Ca are significantly  
107 elevated in pre-gametogenic foraminifers compared to foraminifers that underwent  
108 gametogenesis; B/Ca was found to be higher by  $\sim 15 \mu\text{mol}/\text{mol}$  (23%), while Mg/Ca was  
109 elevated by  $\sim 4 \text{ mmol}/\text{mol}$  (42%, Figure S2). Given the increase observed in both  
110 elemental ratios, this may suggest that gametogenic calcite has a lower concentration of  
111 impurities; however, a consistent decrease in B/Ca and Mg/Ca towards the outside of the  
112 shell is not observed in laser ablation profiles (e.g. Holland et al. 2017). Nevertheless,  
113 this implies that combining gametogenic and pre-gametogenic foraminifera in trace  
114 elemental analyses can significantly bias trace element results, with the effect being  
115 larger for Mg/Ca than B/Ca.

116

117  
118  
119  
120  
121  
122  
123  
124  
125  
126  
127  
128  
129  
130



131 Figure S2. The effect of using terminated versus gametogenic foraminifers in trace  
132 element analyses. Foraminifers that were terminated prior to gametogenesis had  
133 significantly higher B/Ca (red) and Mg/Ca (blue) than GAM foraminifers from the same  
134 experiment. Error bars are  $2\sigma$ . Errors on Mg/Ca (0.8%) are too small to be observed in  
135 this plot.

136  
137  
138  
139  
140  
141  
142  
143  
144  
145  
146  
147  
148  
149  
150  
151  
152  
153  
154  
155  
156

Based on the pre-cleaning weight of the one pre-gametogenic foraminifer we included, it could at maximum have contributed 9% of the total shell sample weight. However, given that pre-gametogenic shells include a much greater amount of organic matter than shells that have undergone gametogenesis, it is likely that the actual shell weight contribution was much lower (<5%). Nevertheless, we must consider whether this contribution could have biased our results. If pre-gametogenic foraminiferal calcite were a significant contributor to the bulk signal, both B/Ca and Mg/Ca could be elevated above the true value of gametogenic specimens. This is difficult to determine for B/Ca in low light experiments, as we anticipated that low light conditions would decrease B/Ca, while a contribution of pre-gametogenic foraminiferal calcite would increase it, effectively canceling out the low light signal. In contrast, we would expect that both low light conditions and contributions of pre-gametogenic foraminiferal calcite would increase Mg/Ca; thus, a pre-gametogenic calcite signature would amplify the low light signal. However, we do not see any increase in shell Mg/Ca in low light experiments on Santa Catalina Island compared to Mg/Ca from the ambient high light experiments of Allen et al. (2011, reported in Allen et al. 2016, Figure 7a, Table 2). Consequently, this result supports the observation from location specific B/Ca calibrations that the sensitivity of foraminiferal symbiont photosynthesis to low light is diminished on Santa Catalina Island (see main text), and that pre-gametogenic foraminiferal calcite was not a significant major contributor to our bulk shell signal.

157

#### 158 **S4. Calculating Calibration Line Parameters & Uncertainty**

159 All linear fits in this study were calculated using the York\_Fit.m script in MatLab (Travis  
160 Wiens 2010, from York et al. 2004). Uncertainty on calibration slopes and intercepts  
161 were calculated as follows:

162  $1\sigma$  uncertainty in seawater- $[\text{B}(\text{OH})_4^-]$  and DIC calculated in CO2sys.m (see eq. 3 in the  
163 manuscript) was used to calculate  $1\sigma$  uncertainty in the  $[\text{B}(\text{OH})_4^-]/\text{DIC}$  ratio for each  
164 experiment according to the following error propagation equation:

165

$$166 \quad \text{Eq. S1} \quad 1\sigma_{[\text{B}(\text{OH})_4^-]/\text{DIC}} = [\text{B}(\text{OH})_4^-/\text{DIC}] * \sqrt{\left(\frac{\sigma_{\text{Borate}}}{\text{Borate}}\right)^2 + \left(\frac{\sigma_{\text{DIC}}}{\text{DIC}}\right)^2}$$

167

168  $1\sigma$  values for  $[\text{B}(\text{OH})_4^-]/\text{DIC}$  and measured B/Ca were entered into the York\_Fit.m script  
169 to calculate resultant  $1\sigma$  uncertainties on calibration slope and intercept.  $2\sigma$  uncertainties  
170 are reported in Table 2.

#### 171 **S5. Shifting Calibration Curves through pre-PETM Conditions**

172 To apply our calibrations to the B/Ca data measured at the PETM in *M. velascoensis*  
173 (Penman et al. 2014), we calculated new intercepts for each calibration to pass through  
174 the pre-PETM average B/Ca and  $[\text{B}(\text{OH})_4^-]/\text{DIC}$  conditions (Table 3). Average measured  
175 pre-PETM B/Ca was  $70.4 \mu\text{mol/mol}$  (Penman et al. 2014). We calculate average pre-  
176 PETM  $[\text{B}(\text{OH})_4^-]/\text{DIC}$  by parameterizing the CO2SYS.m script with the  $\delta^{11}\text{B}$ -derived pre-  
177 event pH data (assuming a pre-PETM pH of 7.8) and T and S trajectories of Penman et  
178 al. (2014), assuming DIC was constant at  $2000 \mu\text{mol kg}^{-1}$ .  $[\text{B}(\text{OH})_4^-]/\text{DIC}$  values for all  
179 pre-PETM data were averaged to find the pre-event condition ( $[\text{B}(\text{OH})_4^-]/\text{DIC}=0.032$ ).  
180 We then passed our calibrations through the average pre-PETM condition ( $70.4$   
181  $\mu\text{mol/mol}$  B/Ca,  $0.032 [\text{B}(\text{OH})_4^-]/\text{DIC}$ ) to find the intercept appropriate for application to  
182 the Paleocene data.

#### 183 **S6. Application to the PETM**

##### 184 *1. Predicted B/Ca at the PETM*

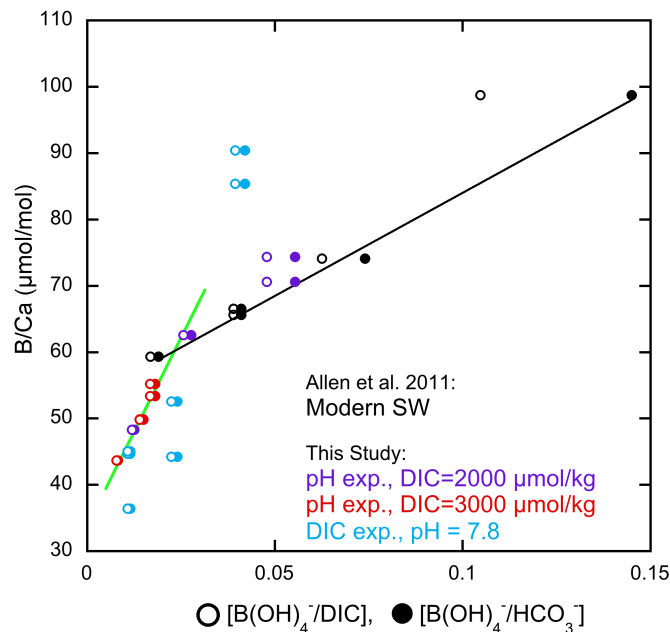
185 In Section 4.4, we predict the B/Ca excursion that we expect to result from the pH  
186 excursion of Penman et al. (2014) given the B/Ca vs. pH calibrations of Allen et al.  
187 (2011, modern seawater) and this study (simulated Paleocene seawater). We use  $\delta^{11}\text{B}$ -  
188 derived pH estimates across the PETM to calculate the associated change in  $[\text{B}(\text{OH})_4^-]$   
189  $]/\text{DIC}$  values across the event using the CO2SYS.m script in Matlab, modified for the  
190 parameterization of  $[\text{B}]_{\text{T}}$ ,  $[\text{Mg}]$ , and  $[\text{Ca}]$ . In the CO2SYS.m script, two carbonate system  
191 input parameters, such as total DIC, alkalinity, or pH, are needed. In our calculations, we  
192 first assume that DIC remained constant at  $2000 \mu\text{mol kg}^{-1}$  and that pH is the only  
193 parameter that changed (decreased) across the PETM. Temperature and salinity were  
194 parameterized according to Penman et al. (2014), where temperature estimates were

195 derived from Mg/Ca measurements on *M. velascoensis*. [Mg] and [Ca] were set at 30 and  
 196 20 mmol/kg, (0.6x and 2x modern values), respectively (Table S6).

197 To estimate uncertainty on calculated  $[B(OH)_4^-]/DIC$  values resulting from  
 198 uncertainties in reconstructed pH, we used the absolute value of the uncertainty  
 199 associated the lower pH bound. This is because the uncertainty in pH estimates is non-  
 200 linear, and the lower uncertainty is thus a larger, most conservative estimate. We ran the  
 201 mean pH value + this  $1\sigma$  uncertainty in pH estimates through the same CO2SYS.m script  
 202 and multiplied by two to find the resultant  $2\sigma$  uncertainty on  $[B(OH)_4^-]/DIC$ . To predict  
 203 B/Ca values, we applied both the modern (Allen et al. 2011) and “Paleocene” calibrations  
 204 (this study, below) (Figure 8, Figure S5):

$$Eq. S2 \quad B/Ca \left( \frac{\mu\text{mol}}{\text{mol}} \right) = 1147 \times \left( \frac{B(OH)_4^- \left( \frac{\mu\text{mol}}{\text{kg}} \right)}{DIC \left( \frac{\mu\text{mol}}{\text{kg}} \right)} \right) + 33.5$$

205 As noted in the main text, using the  $[B(OH)_4^-]/DIC$  ratio over the  $[B(OH)_4^-]/HCO_3^-$  ratio  
 206 does not alter our interpretation, as the calibration sensitivity is the same (Figure S3).  
 207 This is because DIC is primarily composed of  $HCO_3^-$  in our experimental pH range.



224 Figure S3. Paleocene and Modern B/Ca calibrations vs.  $[B(OH)_4^-]/DIC$  (open symbols)  
 225 and  $[B(OH)_4^-]/HCO_3^-$  (closed symbols). Paleocene data from this study is shown in  
 226 colored symbols. The assumption that  $[B(OH)_4^-]/DIC$  is the controlling parameter on  
 227 B/Ca instead of  $[B(OH)_4^-]/HCO_3^-$  does not change the observed increase in sensitivity at  
 228 low pH and high DIC in Paleocene experiments. Linear regression lines for modern pH  
 229 experiments (black) and Paleocene low pH/high DIC experiments (green) are shown.

230

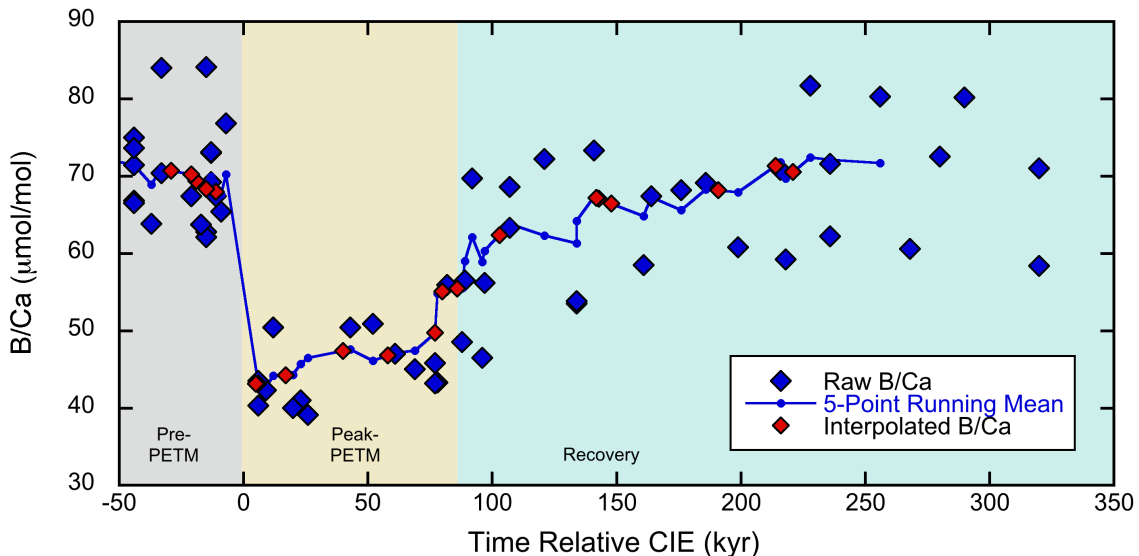
231 Uncertainty in predicted B/Ca was estimated in MatLab by creating random  
 232 variables of N=1000 with mean and standard deviation of calculated  $[B(OH)_4^-]/DIC$  (as  
 233 above), calibration slope, and intercept. The uncertainty associated with the intercept that  
 234 we use in our calibration was the  $1\sigma$  value of pre-PETM B/Ca measurements, which is  
 235 what we used to calculate the intercept (average = 70.4 +/- 1.4, see section E above).  
 236 Each random variable was propagated through the above calculation to find the resultant  
 237  $2\sigma$  uncertainty in predicted B/Ca due to the uncertainty associated with each parameter.  
 238 To find total uncertainty for each predicted B/Ca point, an error propagation was  
 239 performed according to the following equation, to combine uncertainties in calculated  
 240 B/Ca due to each input parameter uncertainty:

$$Eq. S3 \quad 2\sigma_{Predicted\ B/Ca} = \sqrt{(2\sigma)_{\frac{borate}{DIC}}^2 + (2\sigma)_{intercept}^2 + (2\sigma)_{slope}^2}$$

241 **2. Calculating DIC at the PETM**

242 We use our “Paleocene” calibration for B/Ca versus both pH and DIC at  $[B(OH)_4^-]/DIC <$   
 243 0.03 to calculate the DIC increase required to explain the full B/Ca excursion at the  
 244 PETM (Eq. S2). To solve for DIC, we need: 1) Estimates of  $[B(OH)_4^-]$ , and 2) measured  
 245 B/Ca data at the same time points. Data for this calculation come from Penman et al.  
 246 (2014), where B/Ca was measured at site 1209 in *M. velascoensis*, and a  $\delta^{11}B$  pH  
 247 reconstruction from the same site gives us  $[B(OH)_4^-]$  estimates (calculated in CO2SYS.m  
 248 as above).

249 However, B/Ca and  $\delta^{11}B$  were not measured on the same samples, so we must  
 250 interpolate B/Ca data to the time points when  $\delta^{11}B$  was measured. To do this, we firstly  
 251 created a 5-point running mean of measured B/Ca values in *M. velascoensis* (Penman et  
 252 al. 2014, Table S6, Figure S4). Where multiple measurements were made at a single time  
 253 point, measurements from that time interval were averaged before creating the running  
 254 mean. To preserve the discrete interval of the PETM from averaging, we created two  
 255 running mean sections, one each for the pre- and post-CIE, each using the CIE as the  
 256 average starting point. We then linearly interpolated our 5-point running mean values to  
 257 the time points of  $\delta^{11}B$  measurements (Figure S4).



269 Figure S4. 5-point running mean (blue dots & line) of measured B/Ca from Penman et al.  
 270 (2014, blue diamonds) and linear interpolation to time points where  $\delta^{11}\text{B}$  was measured  
 271 (red diamonds).

272  
 273

We then calculate DIC by re-arranging our calibration equation as follows:

$$Eq. S4 \quad DIC \left( \frac{\mu\text{mol}}{\text{kg}} \right) = \frac{B(OH)_4^- \left( \frac{\mu\text{mol}}{\text{kg}} \right)}{(B/Ca \left( \frac{\mu\text{mol}}{\text{mol}} \right) - 33.5)/1147}$$

274 While our experimental conditions only extended to  $4000 \mu\text{mol kg}^{-1}$  DIC, we assume that  
 275 our calibrations extend linearly beyond this point to calculate maximum DIC.

276 To calculate  $\Omega_{\text{calcite}}$  associated with this calculated DIC excursion, we used the  
 277 CO2SYS.m script to solve for the carbonate system at each time point (Table S6). We  
 278 used the same T, S, and pH parameterizations as in the descriptions above, and varied  
 279 DIC according to our calculated values.

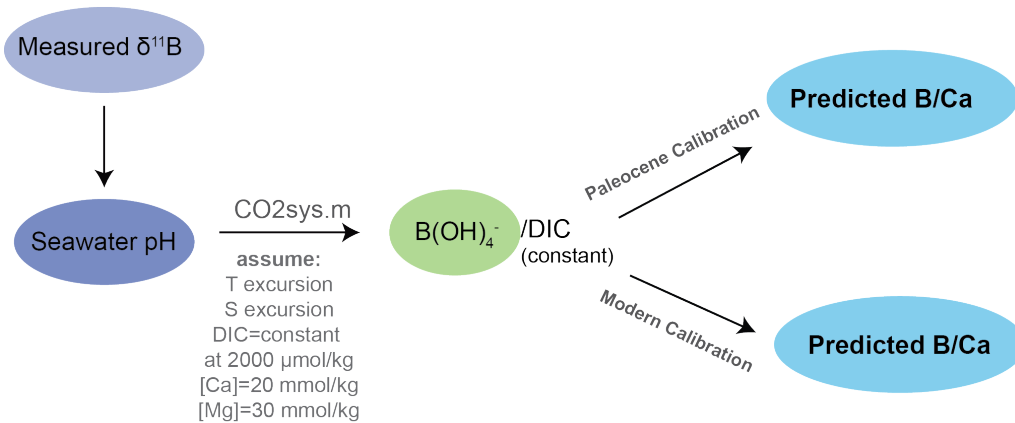
280

**Step 1. How much should B/Ca decrease across the PETM?**

281  
 282

Assuming B/Ca only depends on pH, predict the B/Ca excursion that should result from the  $\delta^{11}\text{B}$ -derived pH decrease using modern & Paleocene pH calibrations.

283



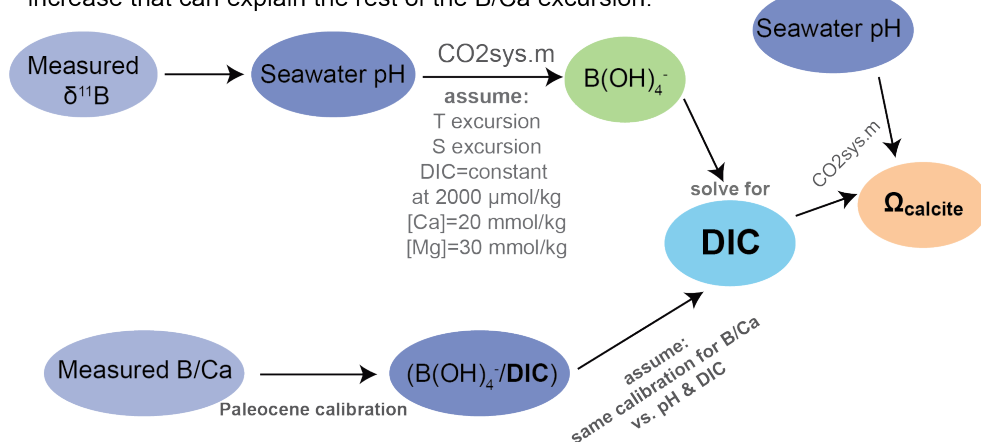
289  
 290  
 291  
 292  
 293

**Step 2. How much DIC is needed to explain the rest of the excursion?**

294  
 295

Assume pH (and thus  $B(OH)_4^-$ ) decreases according to  $\delta^{11}\text{B}$ , and solve for the DIC increase that can explain the rest of the B/Ca excursion.

296



297  
 298  
 299  
 300  
 301  
 302  
 303  
 304

305 Figure S5. Schematic for PETM carbonate chemistry calculations. The calibration or  
 306 assumptions used in each calculation step are shown in grey. Steps where the CO2sys.m  
 307 Matlab script was used to calculate the carbonate system are noted.

308

309 *3. Alternate Calibration Scenario*

310 In our highest DIC experiment, two replicates show good reproducibility while one is  
 311 significantly lower by about 10  $\mu\text{mol/mol}$  (Figure 3, Figure S6, see main text for details).  
 312 We investigate the alternate calibration scenario in which we include this lower replicate  
 313 in our linear regression. Including this data point in our regression increases the  
 314 sensitivity of our calibration (slope  $m= 1495 \pm 302$  versus  $1147 \pm 283$ ), though the two  
 315 are within  $2\sigma$  uncertainty of each other. We explore the implications of using the more  
 316 sensitive calibration for application to PETM data in Figure S7. When the one low  
 317 replicate is included in the calibration, it decreases the reconstructed  $\Delta\text{DIC}$  excursion to  
 318  $\sim+1000 \mu\text{mol kg}^{-1}$ , compared to the  $\sim+2500 \mu\text{mol kg}^{-1}$  increase observed when the  
 319 replicate is not included. In addition, calculated  $\Omega_{\text{calcite}}$  no longer significantly increases in  
 320 this scenario, which is more consistent with the notion of PETM surface ocean  
 321 acidification (Penman et al. 2014) than a large increase in  $\Omega_{\text{calcite}}$ .

322

323

324

325

326

327

328

329

330

331

332

333

334

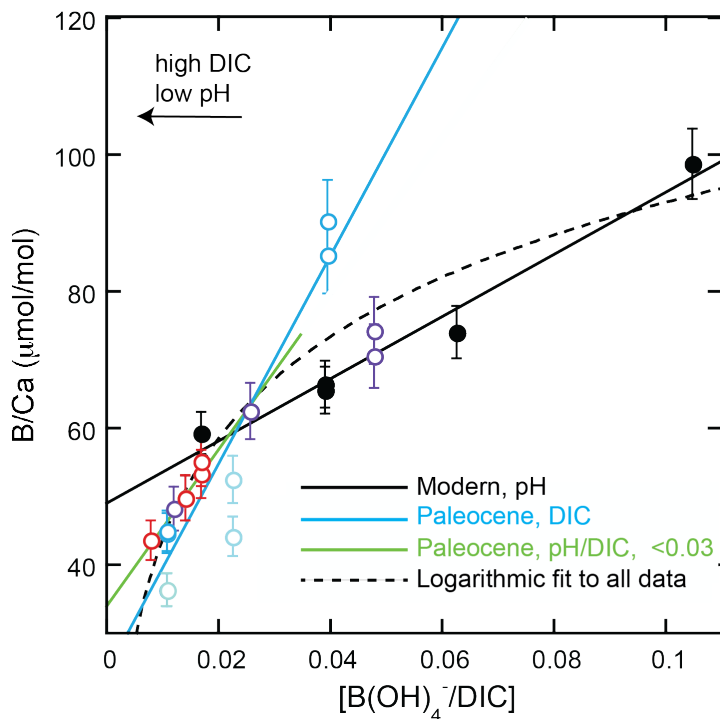
335

336

337

338

339



340

341

342

343

344

Figure S6. Scenarios for calibration fits to modern and Paleocene B/Ca culture data. The modern seawater data of Allen et al. (2011) are shown in black. pH experiments at constant DIC= 2000  $\mu\text{mol kg}^{-1}$  (purple circles) and 3000  $\mu\text{mol kg}^{-1}$  (red circles) are shown as in main text Figure 3. DIC experiments (at constant  $\text{pH}_{\text{Tot}}=7.8$ ) are shown in blue with a linear fit added. The green line is a linear fit to all data where  $[\text{B}(\text{OH})_4^-]/\text{DIC}$

345 <0.03, excluding the DIC=2063  $\mu\text{mol kg}^{-1}$  experiment and the DIC=4000  $\mu\text{mol kg}^{-1}$   
346 replicate that is lower (light blue circles). A logarithmic fit to all of the data is shown in  
347 the dashed line. While the fit appears to explain the data when  $[\text{B}(\text{OH})_4^-]/\text{DIC}<0.03$ , at  
348  $[\text{B}(\text{OH})_4^-]/\text{DIC}>0.03$  pH and DIC experiments diverge, precluding a simple singular fit to  
349 the data.

350

351

352

353

354

355

356

357

358

359

360

361

362

363

364

365

366

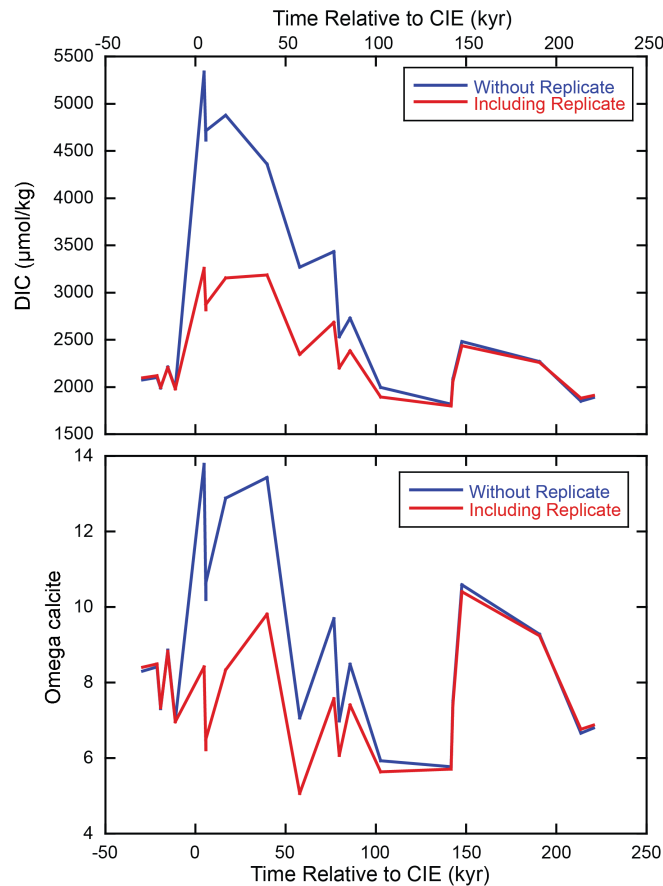
367

368

369

370

371



372

373

374

375

376

Figure S7. Reconstructed DIC and  $\Omega_{\text{calcite}}$  using two formulations of the Paleocene B/Ca calibration. The blue line shows the case where the lower replicate from our highest DIC experiment (LH5) is not included. The red line shows the reconstructions when the replicate is included, and calibration sensitivity drastically increases.

377

378

379

380

381

382

383

384

This result illustrates that by calibrating only one foraminifera species for the “Paleocene”, the calibration uncertainties on reconstructing  $\Delta\text{DIC}$  or  $\Omega_{\text{calcite}}$  at the PETM are rather large for quantitative application; a small change in calibration formulation has the capacity to change the overall interpretation of the record entirely. Consequently, calibration of other symbiont-bearing species is necessary to reduce the uncertainty on PETM ocean acidification estimates, and to further confirm the effect we observe at low  $[\text{B}(\text{OH})_4^-]/\text{DIC}$  in the one species (*O. universa*) that we studied herein.

385 **Supplementary Tables.**

386

387 Table S1. Brunauer-Emmett-Teller Measurements of pooled fossil *O. universa* shell

388 surface area (SSA).

Size Fraction ( $\mu\text{m}$ )	Avg. SSA ( $\text{m}^2/\text{g}$ )	Number of shells included	Average Individual Shell Weight (mg)	Average Individual SSA ( $\text{m}^2$ )
425 - 515	4.3	380	0.037	0.000158
515 - 600	4.3	110	0.055	0.000235
600 - 865	4.7	216	0.078	0.000369

389 Table S4. B/Ca and Mg/Ca data of foraminifers at different life cycle states.

390

391

392

393

394

395

396

Sample	Life cycle state	B/Ca $\mu\text{mol}/\text{mol}$	$2\sigma$	Mg/Ca $\text{mmol}/\text{mol}$	$2\sigma$
BH7a	Not Gametogenic	91	6	11.71	0.09
BH7b	Gametogenic	74	5	8.20	0.07
<b>% Change</b>		<b>24</b>		<b>43</b>	

397 Table S5. p-values for the null hypothesis that shell weights and growth rate are

398 uncorrelated with experimental parameters.

Variable	p value	
	Shell Wt. ( $\mu\text{g}$ )	$\mu\text{g}/\text{day}$
[Ca]	0.25	0.88
[B]t	0.16	0.79
DIC	0.009*	0.28
pH	0.18	0.18

\*denotes significance at a 90% confidence level.

399

400

401